

# Monitoring the Impacts of Government Interventions to Contain COVID-19: A Quantitative Approach

Shuo Wang<sup>1#</sup>, Xian Yang<sup>1,2#</sup>, Yuan Huang<sup>3</sup>, Ling Li<sup>4</sup>, Zhongzhao Teng<sup>5</sup> and Yike Guo<sup>1,6\*</sup>

<sup>1</sup>Data Science Institute, Imperial College London, UK

<sup>2</sup>Department Computer Science, Hong Kong Baptist University, Hong Kong Special Administrative Region, China

<sup>3</sup>Department of Pure Mathematics and Mathematical Statistics, University of Cambridge, UK

<sup>4</sup>School of Computing, University of Kent, UK

<sup>5</sup>Department of Radiology, University of Cambridge, UK

<sup>6</sup>Hong Kong Baptist University, Hong Kong Special Administrative Region, China

# Contribute equally

\* Corresponding author: y.guo@imperial.ac.uk

## ABSTRACT

Monitoring the evolving impacts of non-pharmaceutical intervention measures requires fine-grained estimation of transmission dynamics. We propose a framework to estimate instantaneous reproduction number  $R_t$  using Bayesian inference upon a renewal process, disentangling the  $R_t$  reduction into mitigation and suppression factors for quantifying their impacts at a finer granularity. Investigating the impacts of intervention measures of European countries, the United States and Wuhan with the framework, we reveal the effects of interventions in Europe and alert that 30 states in the United States are facing resurgence risks.

## MAIN TEXT

In response to the COVID-19 pandemic, governments have taken non-pharmaceutical intervention measures. Common measures include travel restriction, school and non-essential business closure and social distancing, as well as early isolation of confirmed patients. Recently, as the first-wave epidemic peak has faded away in many countries, the accumulated observations of epidemic growth<sup>1</sup> and corresponding intervention policies<sup>2</sup> shed more insights on how the interventions worked. Meanwhile, many governments have switched into the phase to reopen economic and social activities, with attention on tamping down possible resurgences. It is important to monitor the epidemic evolution while intervention measures are being relaxed. To gain insights into epidemic evolution, most existing studies<sup>3,4</sup> focus on estimating time-varying instantaneous reproduction number  $R_t$ , defined as the average number of secondary cases that would be induced by an infected primary case at a time  $t$  when conditions remained the same thereafter<sup>5</sup>. The aim of intervention measures is to reduce  $R_t$  so that the epidemic can be contained. To monitor the evolving impacts, more fine-grained modelling of the transmission dynamics is required. This includes just-in-time  $R_t$  estimation without fixed time window and interpretation of the time-varying transmission behaviours at a finer granularity. We propose a novel method to estimate instantaneous reproduction number  $R_t$  using Bayesian inference where the impacts of intervention on  $R_t$  reduction is disentangled as: **mitigation** and **suppression**<sup>6</sup> (see Methods). The mitigation factor ( $p_t$ ) captures the effect of shielding susceptible population (e.g. through social distancing), and the suppression factor ( $D_t$ ) captures the effect of isolating the infected population (e.g. through quarantine) to stop virus transmission. The two factors work in distinct ways contributing to the evolution of  $R_t$  under the interventions (Figure 1A).

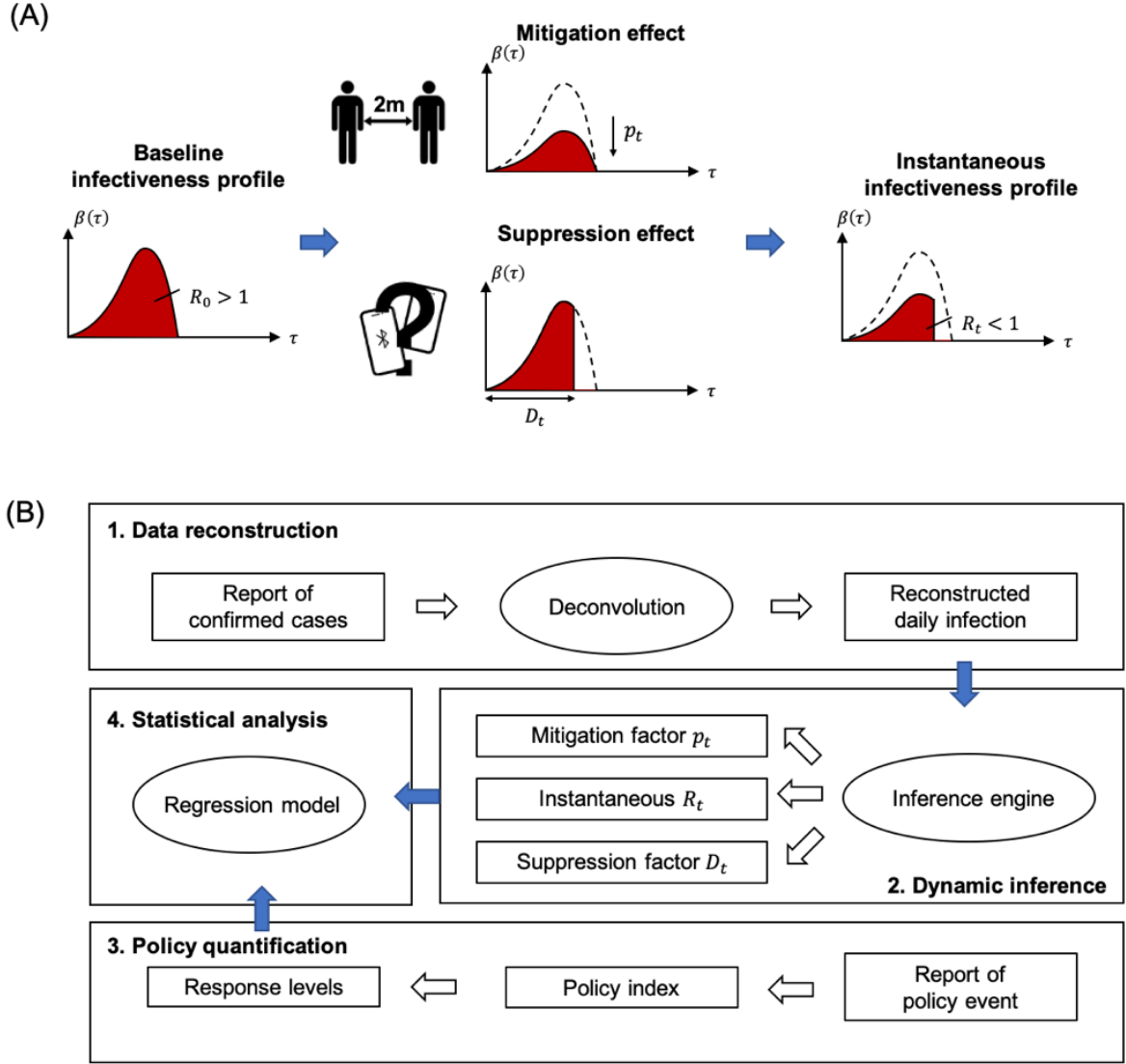


**Figure 1. (A) Disentangling the reduction of reproduction number into mitigation and suppression factors.** The infectiousness profile represents that a primary case who was infected  $\tau$  time ago can generate new secondary cases at a rate of  $\beta(\tau)$ .  $R_t$  is the area under the curve of instantaneous infectiousness profile. The impact of intervention measures on  $R_t$  reduction is disentangled: mitigation factor  $p_t$  attenuates the overall infectiousness through shielding the susceptible population and suppression factor  $D_t$  shortens the infectious period through isolating the infected population. **(B) Components of the quantification framework.** The evolution of mitigation and suppression factors are estimated using the infection data reconstructed from the daily reported confirmed cases. Given the history of government responses, the impacts of intervention measures are quantified by correlating the inferred epidemic parameters to response levels.

A comprehensive framework is then developed to quantify the impacts of different interventions through monitoring the evolution of  $\langle R_t, p_t, D_t \rangle$ . This framework contains data reconstruction, modelling and dynamic inference as shown in Figure 1B. Firstly, we reconstruct the number of daily infections from reports of confirmed cases, taking into account the incubation time and report delay with a deconvolution algorithm. Secondly, we propose a time-varying renewal process with two complementary parameters  $p_t$  and  $D_t$  to model the evolving infectiousness profile. Thirdly, we develop a Bayesian approach for dynamic inference of  $p_t$ ,  $D_t$  and consequent  $R_t$ . We validate the effectiveness of our approach in capturing the sudden change of  $R_t$  evolution induced by interventions, which is hard to be detected by traditional sliding window-based methods (Extended Data Figure 3). Finally, we employ an overall stringency index<sup>2</sup> to characterise the government response levels and assess the impacts of interventions accordingly. The component algorithms and validation of the framework are detailed in Methods.

We have applied the framework to analyse the intervention impacts in many countries. Several examples are illustrated in Figure 2 such as inferring the evolution of  $R_t$  in the United Kingdom (Figure 2A); inferring the immediate effect of a policy in Wuhan (Figure 2B). A retrospective statistical analysis of intervention impacts in 14 European countries is illustrated by Figure 2C and Figure 2D. According to the normalised stringency index by Oxford report<sup>2</sup>, we categorised the dates into five response levels (Level 0:  $S_t \leq 20\%$ , minimal response for reference; Level 1:  $20\% < S_t \leq 40\%$ , soft response; Level 2:  $40\% < S_t \leq 60\%$ , strong response; Level 3:  $60\% < S_t \leq 80\%$  and Level 4:  $80\% < S_t \leq 100\%$ , emergent responses). The representative intervention measures for each response level were identified based on the contribution to the stringency index  $S_t$ .

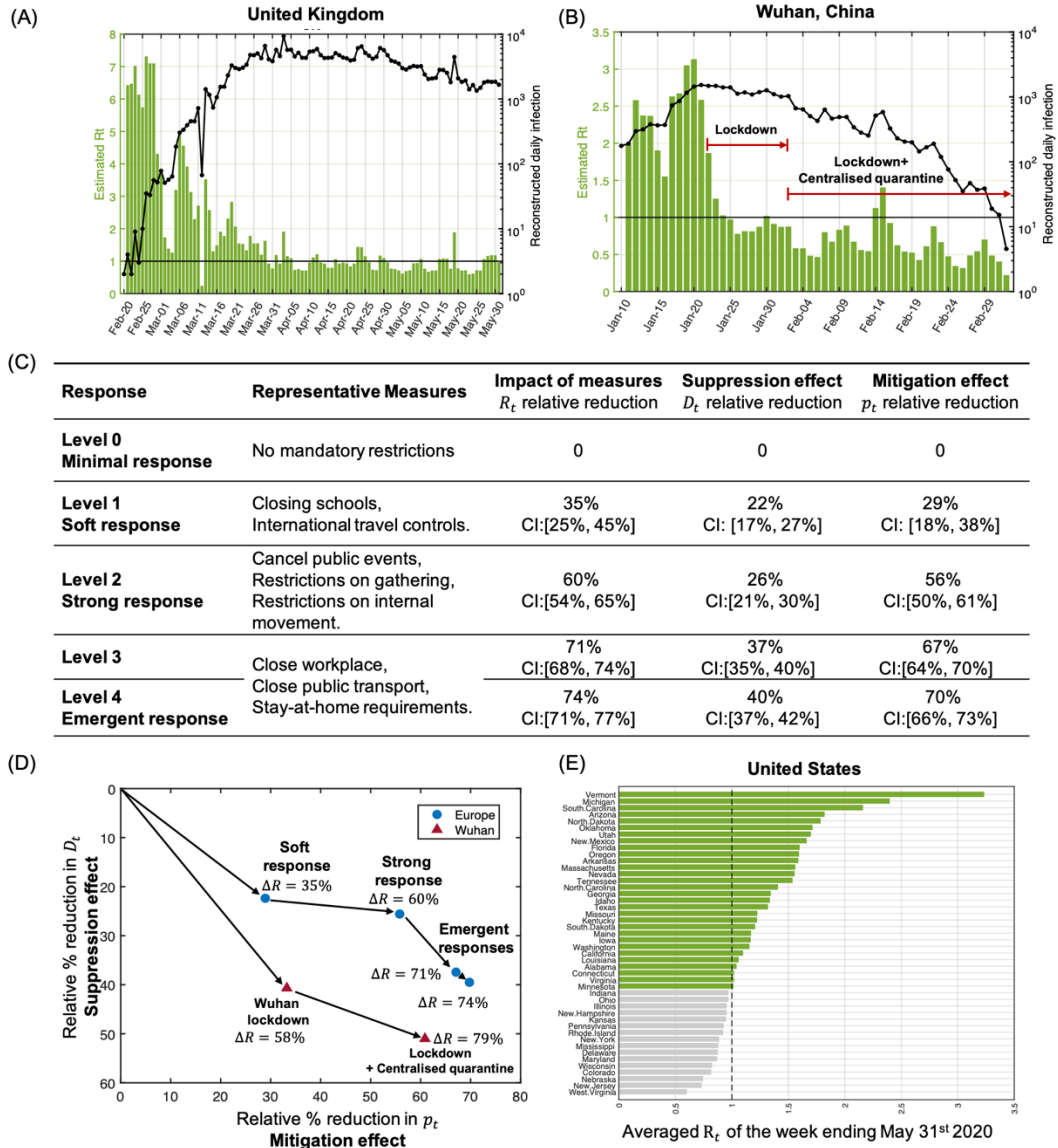


**Figure 2. Retrospective analysis of the impacts of interventions.** The inference results of UK (A) and Wuhan (B) are demonstrated, where the black line represents the reconstructed daily infection number and the green bar is the posterior mean of estimated  $R_t$ . For Wuhan, two major events (city lockdown measure from Jan 23<sup>rd</sup> and centralised quarantine from Feb 2<sup>nd</sup>) are annotated with red arrows (B, D). The implementation of lockdown alone showed a relative  $R_t$  reduction by 58% (CI: [36%, 73%]) compared to  $R_0$ . The combined lockdown and centralised quarantine measures showed more substantial  $R_t$  reduction (79% relative reduction compared to  $R_0$ ). Through statistical analysis of 14 European countries, we estimated the relative reduction of mitigation factor  $p_t$  and suppression factor  $D_t$  under different response levels compared to minimal response level (C, D). Representative intervention measures of each response level are also listed. We report the result of averaged  $R_t$  in the US during the week ending May 31<sup>st</sup> 2020, which is ranked by the averaged  $R_t$  value (annotated with green if above 1) (E). States with total confirmed cases less than 1,000 are excluded from the analysis.

We observed different reduction rates of  $\langle R_t, p_t, D_t \rangle$  for these response levels (Figure 2C). The relative reduction of  $\langle R_t, p_t, D_t \rangle$  compared to the minimal response (Level 0 where  $R_t$  is set to  $R_0$ ) was estimated for each response level. With soft response (Level 1), the corresponding intervention measures (e.g. school closure, quarantine of international arrivals from high-risk regions) are correlated with a relative reduction of  $R_t$  by 35% showing both strong suppression effect ( $D_t$  shortening 22%) and mitigation effect ( $p_t$  reduction 29%). With strong response (Level 2), the relative reduction of  $R_t$  increases to 60% with a strong mitigation effect ( $p_t$  reduction 56%). But the suppression effect ( $D_t$  shortening 26%) is similar to that of Level 1, indicating marginal incremental suppression effect. This observation shows a consistency with the aim of representative intervention measures on this level (e.g. cancelling public events, restrictions on gathering and internal movements) to reduce the contact rates among the population. The emergent response (Level 3) shows substantial relative reduction of reproductive number ( $R_t$  reduction 71%) with suppression ( $D_t$  shortening 37%) and mitigation ( $p_t$  reduction 67%) effects, correlated to the intensive measures (e.g. workplace closure and stay-at-home requirements). A similar degree of reductions is found for Level 4 ( $R_t$  reduction 74%;  $D_t$  shortening 40%;  $p_t$  reduction 70%) while the stringency of intervention measures is higher.

We find that our estimated evolving patterns of  $p_t$  and  $D_t$  correspond well to the serial strategies taken by some European countries, such as the ‘contain-delay-lockdown’ route taken in the UK. Compared to our analysis of Wuhan data, the strong impact of lockdown is clearly demonstrated with the immediate relative reduction of  $R_t$  by 58%. We also observed that the combination of lockdown, centralised quarantine and immediate admission of confirmed patients starting from Feb 2<sup>nd</sup> in Wuhan was associated with a more substantial relative reduction of  $R_t$  with strong suppression and mitigation effects (Figure 2D).

We also used the proposed framework to estimate the epidemic evolution in different states of the United States (Supplementary Table 1). We observed that, as of the week ending May 31<sup>st</sup>, the reproduction number  $R_t$  in 30 states exceeds 1 (Figure 2E). These could be related to the recent lift of government restrictions and alert us to take a close monitoring on the epidemic evolution. This alarming prediction is unfortunately proven true. At the time of writing this communication (June 18<sup>th</sup> 2020), 29 out of the 30 states we alerted on 9<sup>th</sup> of June 2020 have experienced increased number of daily confirmed cases compared to that of May 31<sup>st</sup>, and 14 states have recorded all-time high after May 31<sup>st</sup>.

So far, the inferred evolution of  $R_t$  in many countries and the retrospective impact analysis of intervention measures in European countries indicate the effectiveness of our approach in monitoring  $R_t$ . This can be further validated by predicting the  $R_t$  evolution and projected infections in future study. Our current study has several limitations. Firstly, the reporting protocols and standards of confirmed cases, as well as the detection rates, vary among countries. However, as long as the reporting bias is consistent over time, the inference results of  $p_t$ ,  $D_t$  and  $R_t$  should not be affected. We also note that the implementation of multiple intervention measures within a short interval makes it challenging to quantify the impact of a single measure which needs further statistical analysis.

In conclusion, we propose a comprehensive approach to quantify the impacts of interventions on epidemic evolution of COVID-19. We assess the impacts of intervention measures in different response levels using the proposed method, which opens a promising venue to inform policy for better decision-making in response to a possible second-wave outbreak. We release the framework as an open-source package for public use.

## Reference

1. Dong, E., Du, H. & Gardner, L. An interactive web-based dashboard to track COVID-19 in real time. *Lancet Infect. Dis.* **20**, 533–534 (2020).
2. Hale, T., Petherick, A., Phillips, T. & Webster, S. *Variation in government responses to COVID-19*. (2020).
3. Leung, K., Wu, J. T., Liu, D. & Leung, G. M. First-wave COVID-19 transmissibility and severity in China outside Hubei after control measures, and second-wave scenario planning: a modelling impact assessment. *Lancet* **395**, 1382–1393 (2020).
4. Pan, A. *et al.* Association of Public Health Interventions With the Epidemiology of the COVID-19 Outbreak in Wuhan, China. *JAMA* **323**, 1915 (2020).
5. Fraser, C. Estimating individual and household reproduction numbers in an emerging epidemic. *PLoS One* **2**, (2007).
6. Ferguson, N. M. *et al.* *Report 12: The Global Impact of COVID-19 and Strategies for Mitigation and Suppression*. (2020). doi:10.25561/77735
7. Goldstein, E. *et al.* Reconstructing influenza incidence by deconvolution of daily mortality time series. *Proc. Natl. Acad. Sci. U. S. A.* **106**, 21825–21829 (2009).
8. Ferretti, L. *et al.* Quantifying SARS-CoV-2 transmission suggests epidemic control with digital contact tracing. *Science* **6936**, 1–13 (2020).
9. Thompson, R. N. *et al.* Improved inference of time-varying reproduction numbers during infectious disease outbreaks. *Epidemics* **29**, (2019).
10. Mark, C. *et al.* Bayesian model selection for complex dynamic systems. *Nat. Commun.* **9**, (2018).
11. Agresti, A. *An introduction to categorical data analysis*. (John Wiley & Sons, 2018).



## Methods

**Data Source.** We use the aggregated data of publicly available daily confirmed cases of 14 Europe countries (Austria, Belgium, Denmark, France, Germany, Ireland, Italy, Netherlands, Norway, Portugal, Spain, Sweden, Switzerland and the United Kingdom) and 52 states of the United States from John Hopkins University database<sup>1</sup>. The data include the time series of confirmed cases from January 22<sup>nd</sup> to June 8<sup>th</sup> 2020 (Supplementary Table 2, accessed on June 9<sup>th</sup> 2020). Six states with accumulated confirmed cases less than 1,000 are excluded from the analysis. The daily number of onset patients in Wuhan is adopted from the retrospective study by Pan et. al. <sup>4</sup> The data of intervention measures in European countries are collected from the Oxford Coronavirus Government Response Tracker<sup>2</sup>, reporting the overall stringency index  $S_t$  of intervention measures during the analysis period (Supplementary Table 3, accessed on June 9<sup>th</sup> 2020). This overall stringency index is calculated based on the policy quantification of eight intervention measures (i.e. School closing, Workplace closing, Cancel public events, Restrictions on gatherings, Close public transport, Stay-at-home requirements, Restrictions on internal movement and International travel controls) and one health measure (i.e. public info campaigns) to indicate the government response level of intervention.

**Calculation of intervention policy indices.** We categorise the dates within our analysis period in European countries into five different response levels, based on the overall stringency index  $S_t$ . Level 0 is the reference response level with minimal interventions. To identify the representative measures of each response level, we calculate the quantification indices of eight intervention measures. Descriptions of the eight intervention measures and the quantification methods are provided in Supplementary Table 3. For each intervention measure, the Oxford report provides an ordinal scale quantification  $v_{j,t}$  of the strength of  $j$ -th policy implementation and a binary flag  $f_{j,t}$  representing whether it is implemented in the whole country on time  $t$ .

Following similar practice use in the Oxford report, we normalise the implementation of each intervention measure as

$$P_{j,t} = \frac{\max(0, v_{j,t} + 0.5f_{j,t} - 0.5)}{N_j} \times 100\% \quad (1)$$

where  $N_j$  is the maximum value of the indicator  $P_j$ . To assign a label of response level to each measure, we calculate the change of mean policy indices across different response levels. The response level with largest increase is considered as the level that the measure belongs to (i.e. the measure is a representative measure of this response level). For example, the mean index of school closure showed the largest increase from Level 0 to Level 1, so we consider this is a representative measure of Level 1. The representative measures of each response level are listed in Figure 2C.

**Reconstruction of daily infection from reported cases.** In order to assess the impacts of intervention measures, we need to estimate the time-varying evolution of COVID-19 transmission (e.g. instantaneous reproduction number  $R_t$ ). The observations we have are from the reported number of confirmed cases. However, such observations experience an inevitable time delay between the actual infection time and the reporting date. This includes an incubation time (i.e. the period between infection and onset of symptoms) and confirmation period (i.e. the period between onset and officially reported after test). The confirmed cases reported on time  $t$  were actually infected within a past period and the reported number is the convolution result of the historical daily infection. Here, we reconstruct the daily infection from the confirmed cases using the deconvolution technique with Richardson-Lucy (RL) iteration method<sup>7</sup>. We use the incubation period calculated by Ferretti et al.<sup>8</sup>, which is a lognormal distribution with a mean of 5.5 days and a standard deviation of 2.1 days. We use the confirmation period previously reported by Leung et al.<sup>3</sup>, which is a gamma distribution with a mean of 4.9 days and a standard deviation of 3.3 days. Sampling from these two sequential

distributions, we estimated the interval distribution  $s(\tau)$  from infection to report (Extended Data Figure 1). Denoting the epidemic curve of reported infection cases  $\hat{I}_{1:t} = \{\hat{I}_1, \hat{I}_2, \dots, \hat{I}_t\}$  and the epidemic curve of confirmed cases  $C_{1:t} = \{C_1, C_2, \dots, C_t\}$ , the reported infection with an observation process of past infections can be modelled as a Poisson process:

$$C_t \sim \text{Poisson}(\text{mean} = \sum_k s(k) \hat{I}_{t-k}) \quad (2)$$

Estimate the daily reported infection curve  $\hat{I}_{1:t}$  given the daily confirmed cases curve  $C_{1:t}$  and infection-to-confirmed time distribution  $s_{1:d}$  is an ill-posed deconvolution problem and can be solved using Richardson-Lucy (RL) iteration method<sup>7</sup>. The initial guess  $\hat{I}_{1:t}^0$  is the confirmed cases curve  $C_{1:t}$  shifted back by the mode of the infection-to-confirmed time distribution. Let  $\hat{C}_i^n = \sum_k s(k) \hat{I}_{t-k}^n$  be the expected number of confirmed cases on day  $i$  of iteration  $n$ . Then the iteration of  $\hat{I}_t$  is computed by an expectation-maximization (EM) algorithm as:

$$\hat{I}_t^{n+1} = \hat{I}_t^n \sum_{i>t} \frac{s(i-t)C_t}{\hat{C}_t^n} \quad (3)$$

A normalised  $\chi^2$  statistics is used as the stop criterion of the iteration:

$$\chi^2 = \frac{1}{N} \sum_t \frac{(\hat{C}_t^n - C_t)}{\hat{C}_t^n} < 1 \quad (4)$$

The reconstructed daily infections of the countries in this study is provided in Supplementary Table 4. It is of note that the reported number of confirmed cases constitute the lower bound of the real infection due to the lack of mass test and the existence of asymptomatic cases. However, as long as the detection rate remains consistent, the scaling of reconstructed data does not affect the following inference of transmission dynamics.

**Epidemic modelling of COVID-19 transmission.** To characterise the evolution of COVID-19 transmission, we adopted a time-varying renewal process for epidemic modelling. The renewal process<sup>5</sup> of infectious disease transmission is:

$$I(t) = \int_0^\infty I(t - \tau) \beta(\tau) d\tau \quad (5)$$

where  $I(t)$  is the incident infection on time  $t$  and  $\beta(\tau)$  is the infectiousness profile. The infectiousness profile means a primary case who was infected  $\tau$  time ago can now generate new secondary cases at a rate of  $\beta(\tau)$ , describing a homogenous mixing process. The infectiousness profile  $\beta(\tau)$  is related to biological, behavioural and environmental factors. We can calculate the reproduction number  $R$  as the area under curve (AUC) of  $\beta(\tau)$ , which is the overall number of secondary cases infected by a primary case. Further,  $\beta(\tau)$  can be rewritten as:

$$\beta(\tau) = R \cdot w(\tau) \quad (6)$$

where the unit-normalised transmission rate  $w(\tau)$  is the probability density function of generation time, i.e. the interval between the primary infection and the secondary infection. In the early stage without intervention, the infectiousness profile remains time-independent as the baseline  $\beta_0(\tau)$  which describes the transmission dynamics without interventions. The corresponding  $R$  is the well-known basic reproduction number  $R_0$ . In reality, the infectiousness profile  $\beta_t(\tau)$  will evolve with time caused by intervention measures. To quantify the impacts of intervention measures to the evolution of  $R_t$ , we propose two factors: suppression and mitigation to disentangle the intervention effects. Here we use two complementary metrics  $p_t$  and  $D_t$  modelling the suppression and mitigation factors respectively, as illustrated in Figure 1. The suppression effects mainly shorten the infectious period of the infected population, corresponding to the truncation of  $\beta(\tau)$  along the x-axis. We use a time-varying parameter  $D_t$

to denote the effective infectious window induced by suppression. The mitigation effects attenuate the overall infectiousness by shielding the susceptible population, corresponding to the scaling on the y-axis. We use another time-varying parameter  $p_t$  to describe this attenuation effect induced by mitigation. Formally, we parameterise the evolution of the infectiousness profile as:

$$\beta_t(\tau) = \begin{cases} \beta_0(\tau) \cdot p_t & \tau < D_t \\ 0 & \tau \geq D_t \end{cases} \quad (7)$$

Accordingly, the instantaneous reproductive number  $R_t$  can be derived:

$$R_t = p_t \cdot \int_0^{D_t} \beta_0(\tau) d\tau \quad (8)$$

**Dynamic inference of suppression and mitigation factors.** Traditional  $R_t$  estimation methods using a sliding window<sup>9</sup> (e.g. one week) might not capture the sudden change under newly imposed intervention measures, and can be sensitive to the choice of window size. Also, impacts of intervention measures encapsulated in the evolution of the infectiousness profile might not be clearly revealed by  $R_t$  which is an integral quantity. Thus, we propose a new window-free estimation method based on Bayesian inference. For the defined epidemiology renewal process, the daily incident infection  $I_t$  is the state variable and observed from the reconstructed infection data. The evolution of the state  $I_t$  is governed by the renewal process with the time-varying infectiousness profile  $\beta_t(\tau)$ , parameterised with  $p_t$  and  $D_t$ . Here we develop a Bayesian framework to monitor the evolution of  $p_t$  and  $D_t$  using the daily reports of confirmed cases (Extended Data Figure 2). Our inference framework employs a two-level hierarchical model for the inference of time-varying parameters<sup>10</sup>. Let us denote the observed daily incidence of infection till time step  $t$  as  $\hat{I}_{1:t} = \{\hat{I}_1, \hat{I}_2, \dots, \hat{I}_t\}$ . Suppose  $p(\boldsymbol{\theta}_{t-1} | \hat{I}_{1:t-1})$  is the estimated distribution of  $\boldsymbol{\theta} = [p, D]^T$  at time step  $t - 1$ . Under the assumption of consistent

detection rates, the observed daily incidence  $\hat{I}_t$  also satisfies the renewal process. The low-level model predicts the observation (i.e. reconstructed daily infection) given a parameter set through the renewal process:

$$p(\hat{I}_t | \boldsymbol{\theta}_t, \hat{I}_{1:t-1}) \sim \text{Poisson}(\text{mean} = \sum_{k=1}^{t-1} \beta_t(k; \boldsymbol{\theta}_t) \hat{I}_{t-k}) \quad (9)$$

where a Poisson process of observing the infected cases is assumed. This describes the *likelihood* of observing the new incidence data given history observations and parameter value  $\boldsymbol{\theta}_t$ . The high-level model describes the evolution of the model parameters  $p_t$  and  $D_t$  through transforming the joint distribution:

$$p(\boldsymbol{\theta}_t | \hat{I}_{1:t-1}) = T \circ p(\boldsymbol{\theta}_{t-1} | \hat{I}_{1:t-1}) \quad (10)$$

where  $T(\cdot)$  is a transformation function defining the temporal variations of the  $\boldsymbol{\theta}$ . The *prior* knowledge of parameter distribution is transferred to next time step  $t$  by the high-level model  $T$ . Under the scenario without interventions, the parameters  $p_t$  and  $D_t$  fluctuate around the baseline values. Therefore, we can assume a random walk of  $\boldsymbol{\theta}$  in the parameter space as the high-level model. The update of joint parameter distribution is by convoluting with a Gaussian kernel with variance  $\sigma_1$ . When the intervention is introduced on time  $d$ , the random walk of  $\boldsymbol{\theta}$  is altered where the variance of Gaussian kernel will become  $\sigma_2$ . The transformation  $T(\cdot)$  is defined as:

$$T \circ p(\boldsymbol{\theta}) = \begin{cases} p(\boldsymbol{\theta}) * K_{\sigma_1}(\boldsymbol{\theta}) & t < d \\ p(\boldsymbol{\theta}) * K_{\sigma_2}(\boldsymbol{\theta}) & t \geq d \end{cases} \quad (11)$$

where  $K_{\sigma_1}(\boldsymbol{\theta})$  and  $K_{\sigma_2}(\boldsymbol{\theta})$  are the Gaussian kernels before and after the deployment of intervention on time  $d$ . This high-level model includes three hyperparameters: variances before and after intervention:  $\sigma_1$  and  $\sigma_2$ , and the change-point time  $d$ . Let us denote the

hyperparameters  $\boldsymbol{\eta} = [\sigma_1, \sigma_2, d]^T$ . After seen the latest observation  $\hat{I}_t$ , the *posterior* estimation of  $\boldsymbol{\theta}$  is update by the Bayes theorem:

$$p(\boldsymbol{\theta}_t | \hat{I}_{1:t}) = \frac{T \circ p(\boldsymbol{\theta}_{t-1} | \hat{I}_{1:t-1}) \cdot p(\hat{I}_t | \boldsymbol{\theta}_t, \hat{I}_{1:t-1})}{p(\hat{I}_t | \hat{I}_{1:t-1})} \quad (12)$$

The *posterior* are usually intractable but can be approximated through grid-based methods<sup>10</sup>.

Given a set of hyperparameters  $\boldsymbol{\eta}_i$ , the hybrid model evidence can be calculated as:

$$p(\hat{I}_{1:t} | \boldsymbol{\eta}_i) = \int p(\hat{I}_{1:t}, \boldsymbol{\theta}_t | \boldsymbol{\eta}_i) d\boldsymbol{\theta}_t \quad (13)$$

Finally, the posterior estimation  $p(\boldsymbol{\theta}_t | \hat{I}_{1:t})$  can be averaged across the hyperparameter grids weighted by the hybrid model evidence. The posterior mean and confidence intervals of  $p_t$  and  $D_t$  as well as the corresponding  $R_t$  are obtained in a dynamic manner. The *prior* of  $R_0$  at the first time step is set uninformative as a uniformed distribution with the pre-set lower and upper limits (e.g., the upper limit for the European countries is set to 8 in the experiment). The shape of  $\beta_0(\tau)$  is adapted from the distribution of generation time interval  $w(\tau)$  reported by Ferretti et al.<sup>8</sup> We applied the above framework to infer the epidemic evolution in 14 European countries, states in the US and Wuhan city, China (Supplementary Table S1). The proposed Bayesian inference approach is validated and compared to the sliding window-based method<sup>9</sup> in simulation experiments (Extended Data Figure 3). The sharp change of  $R_t$  can be captured immediately by our Bayesian approach while there is a response lag using the sliding window-based method due to the window effect. The codes of the our inference framework is released as an open-source package ([https://github.com/whfairy2007/COVID19\\_Bayesian](https://github.com/whfairy2007/COVID19_Bayesian)).

**Statistical analysis of the intervention impacts in different response levels.** We performed a retrospective analysis of the time-varying transmission dynamics during different response levels in Europe countries. First, the evolution history of  $R_t$  and the overall stringency index

$S_t$  are obtained using the above framework. The stringency index  $S_t$  is categorised into five response levels (Level 0:  $S_t \leq 20\%$ , minimal response for reference; Level 1:  $20\% < S_t \leq 40\%$ , soft response; Level 2:  $40\% < S_t \leq 60\%$ , strong response; Level 3:  $60\% < S_t \leq 80\%$  and Level 4:  $80\% < S_t \leq 100\%$ , emergent responses). We fit a log-linear mixed-effect model, where the logarithm of  $R_t$  is the outcome variable and categorical stringency index is the predictor. The logarithm is used to obtain the intervention impacts on the relative change of  $R_t$ <sup>11</sup>. We performed a partial-pool analysis by assuming the impacts of intervention measure (slopes) share across all selected European countries while the basic reproduction number  $R_0$  (intercept) varies due to environmental and social factors. The regression formula is written as:

$$\ln R_{j,t} = b_0 + \sum_{k=1}^4 b_k * D_{j,k} + \gamma_j + \epsilon \quad j = 1, 2, \dots, 14 \quad (14)$$

where  $R_{j,t}$  is the estimated reproduction number of  $j$ -th country,  $b_0$  is the fixed effect term of  $\ln R_0$  and  $b_k$  is the fixed effects of interventions in response level  $k$ .  $D_{j,k}$  is the dummy variable that takes the value 1 if and only if the response status is at Level  $k$ .  $\gamma_j$  is the random effect term following zero-mean Gaussian which explains the difference of  $\ln R_0$  across countries and  $\epsilon$  is the Gaussian error term. Equation 14 associates the relative changes in  $R$  to the fixed effects of response levels, and can be rewritten into its marginal form as:

$$\ln\left(1 + \frac{R - R_0}{R_0}\right) = \sum_{k=1}^4 b_k * D_k \quad (15)$$

Therefore, the relative change of  $R$  due to the intervention measures in  $k$ -th response level can be derived from  $b_k$  (i.e.  $\Delta R/R_0 = \exp(b_k) - 1$ ). Country-specific  $\ln R_0$  can be estimated as  $b_0 + \gamma_j$  at the Level 0. The statistical analysis is performed using the R package ‘lme4’. The fixed effect is considered significant with P value  $< 0.05$ . The 95% confidence intervals (CI) are estimated using bootstrap method. The assumption of normality is checked by inspecting the

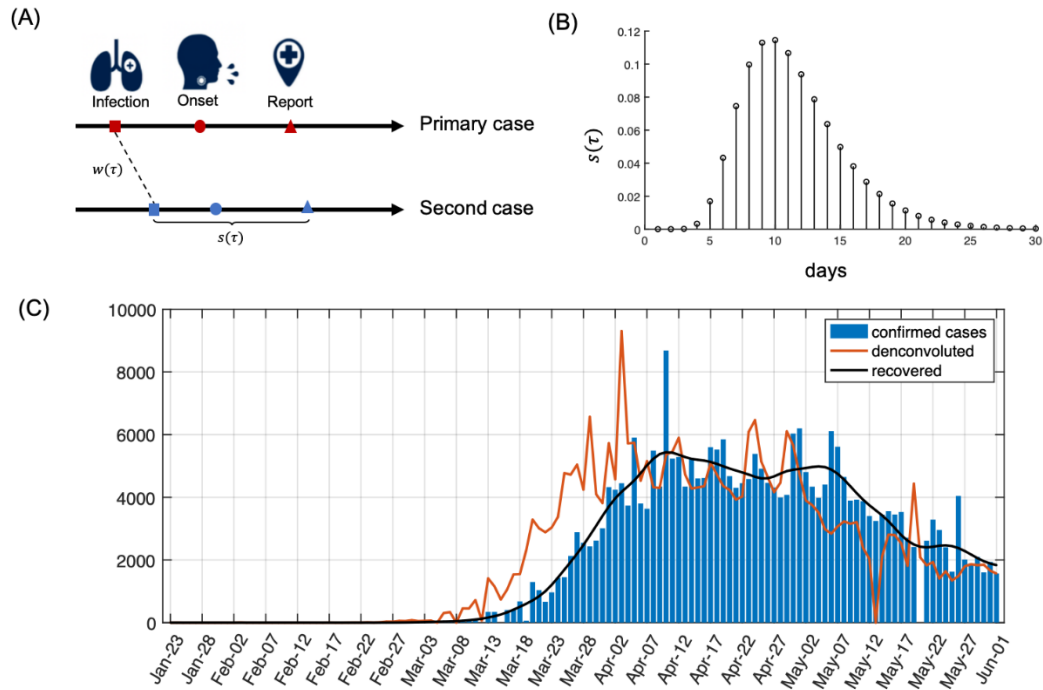


quantile-quantile plot of the residuals. The same procedure is also applied to the analysis of  $D_t$  and  $p_t$  to quantify the suppression and mitigation factors, respectively. The results are demonstrated in Figure 2C and the statistical details are provided in the Supplementary Table 5.

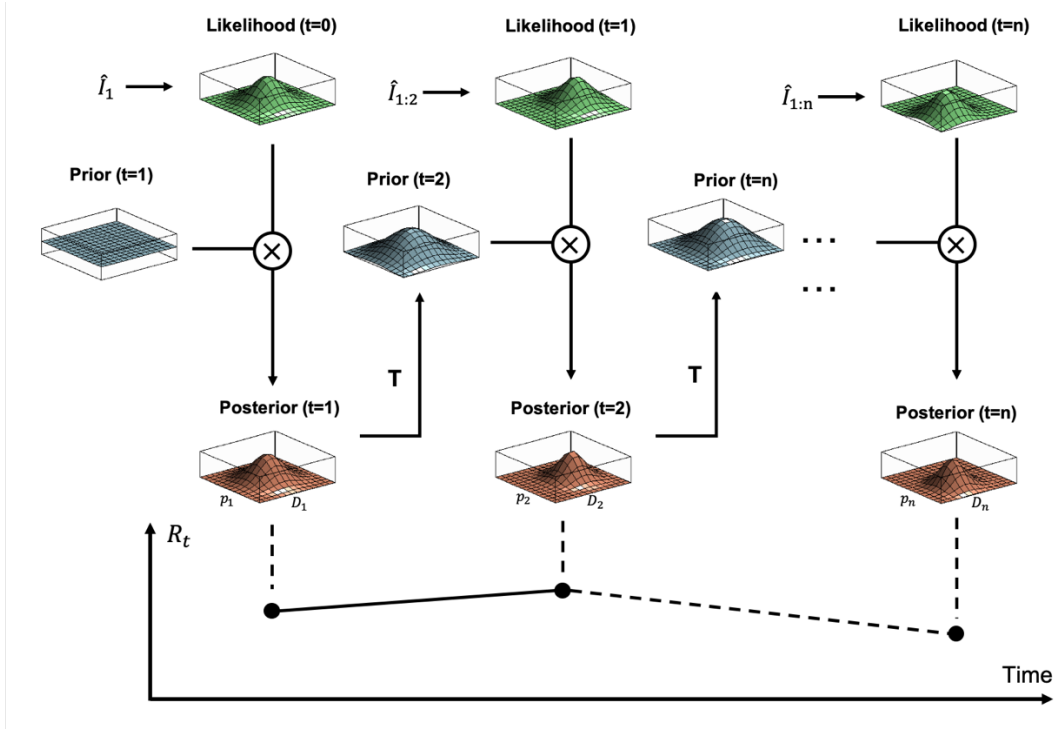
## **Acknowledgement**

We express our sincere thanks to all members of the joint analysis team between Imperial College London, University of Cambridge and University of Kent and Hong Kong Baptist University. We thank Yuting Xing for helping collect epidemic data in Wuhan and the United States. We thank Siyao Wang and Liquun Wu for their efforts on developing digital tracing app for validation and visualisation. We thank Philip Nadler and Rossella Arcucci for insightful discussion on Bayesian inference.

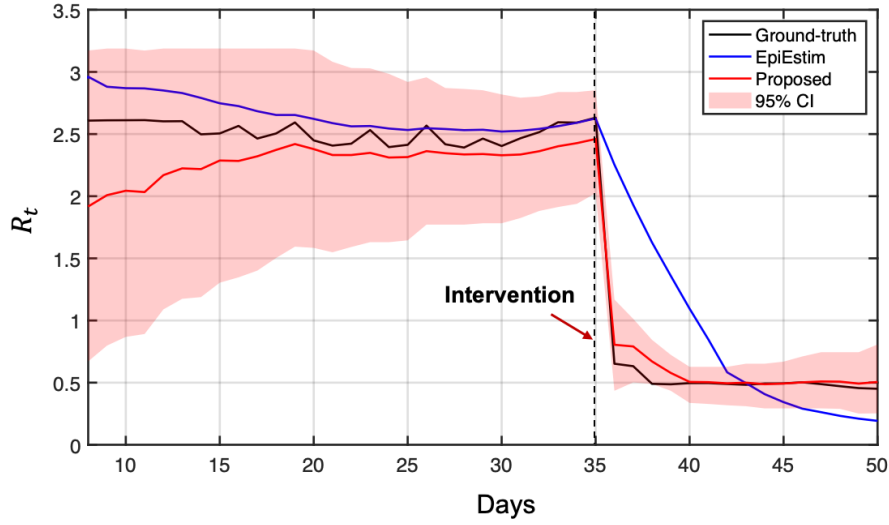
## Supplementary Figures



**Extended Data Figure 1.** Reconstruction of daily infection from the confirmed cases using deconvolution algorithms. The time delay between the infection and onset and report is demonstrated in (A). The estimated distribution between infection and report is presented in (B) which is used for deconvolution. An example of deconvolution results on UK time series is demonstrated in (C) where the forward convolution on reconstructed data matches well with actual reported data, validating the correctness of the method.



**Extended Data Figure 2.** Illustration of the Bayesian inference framework for estimating suppression and mitigation factors. We employ a two-level hierarchical model. For each time step, the low-level model (i.e. renewal process) provides the likelihood of  $p_t, D_t$  (green). The posterior (orange) is calculated through the element product of the likelihood and the prior (blue) from the previous time step. To generate the prior for next time step, we use the high-level model (i.e. the transformation  $T$ ) to induce the evolution of parameters. The high-level model is a piecewise gaussian random walk process where the fluctuations of  $p_t$  and  $D_t$  differ before and after an intervention time. The instantaneous reproduction number  $R_t$  can be derived from the posterior distribution of  $p_t$  and  $D_t$ .



**Extended Data Figure 3.** Validation of the proposed Bayesian inference method. We simulated an artificial epidemic outbreak with time-varying infectiousness profile using renewal process. The generation interval time interval were adapted from Ferretti et al.<sup>8</sup> The simulation period includes 50 days and an intensive intervention measure is induced on day 35 altering the transmission dynamics. Before the intervention, the ground-truth  $R_t$  followed Gaussian random walk with a mean of 2.5. After the intervention (50%  $p_t$  reduction and 67%  $D_t$  reduction), the mean of  $R_t$  was reduced to 0.5 (black line). We compared the results using our approach (red line with 95% confidence intervals) to the results computed by the R package ‘EpiEstim v2.2’<sup>9</sup> (blue) which is a sliding window-based method widely used for  $R_t$  estimation. We observed that the ground-truth  $R_t$  is well estimated within our confidence interval. In particular, the sharp change of  $R_t$  caused by the intervention is captured immediately by our approach while there is a lag using the sliding window-based method.